Title

The 14-3-3 protein PAR-5 regulates the asymmetric localization of the LET-99 spindle positioning protein

Journal

Developmental Biology, 412(2)

ISSN

0012-1606

Authors

Wu, Jui-Ching
Espiritu, Eugenel B
Rose, Lesilee S

Publication Date

2016-04-01

DOI

10.1016/j.ydbio.2016.02.020

Peer reviewed

HHS Public Access

Author manuscript

Dev Biol. Author manuscript; available in PMC 2017 April 15.

Published in final edited form as:

Dev Biol. 2016 April 15; 412(2): 288–297. doi:10.1016/j.ydbio.2016.02.020.

The 14-3-3 Protein PAR-5 Regulates the Asymmetric localization of the LET-99 Spindle Positioning Protein

Jui-Ching Wu[#1], **Eugenel B. Espiritu**[#2], and **Lesilee S. Rose**

Department of Molecular and Cellular Biology, University of California, Davis, USA

[#] These authors contributed equally to this work.

Abstract

PAR proteins play important roles in establishing cytoplasmic polarity as well as regulating spindle positioning during asymmetric division. However, the molecular mechanisms by which the PAR proteins generate asymmetry in different cell types are still being elucidated. Previous studies in *C. elegans* revealed that PAR-3 and PAR-1 regulate the asymmetric localization of LET-99, which in turn controls spindle positioning by affecting the distribution of the conserved force generating complex. In wild-type embryos, LET-99 is localized in a lateral cortical band pattern, via inhibition at the anterior by PAR-3 and at the posterior by PAR-1. In this report, we show that the 14-3-3 protein PAR-5 is also required for cortical LET-99 asymmetry. PAR-5 associated with LET-99 in pull-down assays, and two PAR-5 binding sites were identified in LET-99 using the yeast two-hybrid assay. Mutation of these sites abolished binding in yeast and altered LET-99 localization in vivo: LET-99 was present at the highest levels at the posterior pole of the embryo instead of a band in *par-5* embryos. Together the results indicate that PAR-5 acts in a mechanism with PAR-1 to regulate LET-99 cortical localization.

Keywords

Asymmetric division; PAR-5; LET-99; *C. elegans*; embryo

INTRODUCTION

One mechanism used to accomplish cellular diversity during development is asymmetric division, where a cell divides to produce daughters with different fates. During intrinsically asymmetric divisions, an axis of polarity is established that coordinates two subsequent events. First, cell fate determinants asymmetrically localize with respect to the polarity axis. Second, the mitotic spindle is positioned along the polarity axis to define the site of cleavage so that determinants are differentially segregated to the daughters (reviewed in (Galli and

Address correspondence to Lesilee S. Rose, lsrose@ucdavis.edu, Phone: 530-754-9884, Fax: 530-752-3085.

[1]Present address: Department of Clinical Laboratory Sciences and Medical Biotechnology College of Medicine, National Taiwan University, Taipei, Taiwan 100

[2]Present address: Department of Developmental Biology, University of Pittsburgh, Pittsburgh, PA, 15213, USA

van den Heuvel, 2008; Gonczy, 2008; Morin and Bellaiche, 2011; Rose and Gonczy, 2014; Williams and Fuchs, 2013). Asymmetric divisions are essential for embryonic development as well as for stem cell maintenance and differentiation. Alterations in asymmetric division have also been implicated in tumorigenesis (Florian and Geiger, 2010; Knoblich, 2010; Morin and Bellaiche, 2011; Williams and Fuchs, 2013).

The PAR proteins are conserved from nematodes to mammals and polarize cells by defining specific cortical domains (Galli and van den Heuvel, 2008; Gonczy, 2008; Morin and Bellaiche, 2011; Nance and Zallen, 2011; Rose and Gonczy, 2014; Williams and Fuchs, 2013). In the *Caenorhabditis elegans* one-cell embryo, PAR-3 and PAR-6, and the atypical protein kinase C, PKC-3, localize to the anterior cortex. PAR-2 and the MARK family kinase PAR-1 localize to the posterior cortex. PAR-1 signals through the downstream effectors, MEX-5/6, to generate cytoplasmic asymmetries that define the anterior-posterior (AP) axis and lead to the different cell fates of the daughters of the first division (Galli and van den Heuvel, 2008; Nance and Zallen, 2011; Rose and Gonczy, 2014).

PAR proteins also signal through downstream effectors to position the mitotic spindle on the polarity axis in several systems (Galli and van den Heuvel, 2008; Morin and Bellaiche, 2011; Rose and Gonczy, 2014; Williams and Fuchs, 2013). In *C. elegans* one-cell embryos, the nuclear-centrosome complex undergoes anteriorly-directed centration and rotation movements, such that the spindle forms in the middle of the embryo and is aligned with the AP polarity axis. During metaphase and anaphase, the spindle is displaced posteriorly and the final asymmetric position of the spindle results in unequal division. The PAR proteins control these movements via a force-generating complex at the cortex that includes Gα proteins, two redundant Goloco proteins GPR-1 and GPR-2, and the NuMA family protein LIN-5 (Galli and van den Heuvel, 2008; Morin and Bellaiche, 2011; Rose and Gonczy, 2014; Williams and Fuchs, 2013). As in other systems, the Gα/GPR/LIN-5 complex is thought to recruit the microtubule motor dynein to the cortex, where it acts on astral microtubules to position the spindle (Gonczy, 2008; Kiyomitsu, 2014; Kotak and Gonczy, 2013; Morin and Bellaiche, 2011; Siller and Doe, 2009; Williams and Fuchs, 2013).

To generate nuclear and spindle movements, cortical pulling forces must be asymmetric. Phosphorylation of LIN-5 by PKC-3 facilitates the switch from nuclear centration/rotation to posterior spindle displacement, by inactivating LIN-5 and thus decreasing pulling forces at the anterior cortex (Galli et al., 2011). This regulation is partially redundant with another mechanism that affects LIN-5 and GPR localization and involves LET-99 (Rose and Kemphues, 1998; Tsou et al., 2002; Tsou et al., 2003a). LET-99 localizes to a cortical posterior-lateral band after polarity is established (Tsou et al., 2002). In this region, LET-99 inhibits the cortical localization of GPR-1/2 and LIN-5, thereby inhibiting posterior-lateral pulling forces; in *let-99* mutant embryos, GPR-1/2 and LIN-5 are uniformly distributed at the cortex, which results in symmetric pulling forces and defects in rotation and spindle displacement (Krueger et al., 2010; Park and Rose, 2008; Rose and Kemphues, 1998; Tsou et al., 2003a).

We previously demonstrated that PAR-3 is required to prevent LET-99 accumulation at the anterior cortex, and PAR-1 is needed to inhibit LET-99 from the posterior-most cortex (Tsou

et al., 2002; Wu and Rose, 2007). Cytoplasmic polarity intermediates such as MEX-5/6 are not required for LET-99 localization. Thus, the PAR proteins may regulate LET-99 localization directly, a model that is supported by association of PAR-1 with LET-99, and the requirement of *par-1* kinase activity for normal LET-99 asymmetry (Wu and Rose, 2007).

PAR-5 is another polarity protein that is a member of the 14-3-3 family of proteins. 14-3-3 proteins are involved in many different processes, but in general they act via binding to phosphorylated targets to alter their subcellular localization, activity, or stability (reviewed in (Aristizabal-Corrales et al., 2012; Gardino and Yaffe, 2011; Obsil and Obsilova, 2011). In several systems including *C. elegans* (Morton et al., 2002), orthologs of PAR-5 are required for the mutual exclusion of the PAR proteins from their reciprocal domains. For example, PAR-1 phosphorylates PAR-3 to exclude PAR-3 from the PAR-1 domain in Drosophila oocytes and epithelial cells, in a 14-3-3-dependent manner, while PKC-3 orthologs similarly restricts PAR-1 localization in mammalian epithelial cells (Benton and St Johnston, 2003; Goransson et al., 2006; Suzuki et al., 2004). However, the role of PAR-5 in regulating other downstream targets of PKC-3 and PAR-1 is less studied (Hao et al., 2010; Riechmann and Ephrussi, 2004).

Here we investigate the role of PAR-5 in regulating the asymmetric cortical localization of LET-99. We show that depletion of PAR-5 results in LET-99 expansion into the posterior domain of the one-cell embryo, but LET-99 remains restricted from the anterior cortex. We also show that PAR-5 interacts directly with LET-99 and that predicted 14-3-3 binding sites are required for normal accumulation of LET-99 in a band pattern.

MATERIALS AND METHODS

Worm strains

Worms were cultured on MYOB plates using standard methods (Brenner, 1974; Church et al., 1995). Strains used were as follows: DP38 *unc-119(ed3);* EG6699 *ttTi5605; unc-119(ed3); oxEx1578*); N2, wild-type Bristol variant; RL231 *unc-22(e66) let-99(dd17)* / [qIs51(pha::GFP)] IVRL276, *unc-119(ed3*) III; *unc-22(e66)let-99(dd17)/nT1 [qIs51(pha::GFP)]* IV; RL264, *let-99 (ax218)unc-30 (e1919).* Transgenic strains were maintained at 23-25°C for optimal expression, *let-99(ax218)* at 16°C, and all others at 20°C.

RNA interference

RNA interference by feeding (Timmons and Fire, 1998) was carried out to knock down PAR-5 activity using clone IV-6E06 from the Ahringer RNAi library (Kamath et al., 2003). L4 stage N2 hermaphrodites were placed on plates and incubated at 20°C for 24 hours; depletion of PAR-5 was confirmed by observation of the symmetric division phenotype. N2 fed with bacteria containing vector only were used as controls.

Embryo extract preparation and pull down assays

N2 worms were synchronized at the L1 stage and grown until the early gravid adult stage. Embryos were obtained by hypochlorite treatment (Lewis and Fleming, 1995) and resuspended in lysis buffer (100 mM Tris-HCl pH 7.2, 120 mM NaCl, 1% NP-40, plus

protease and phosphatase inhibitors). The resuspended embryos were frozen with liquid nitrogen, ground to powder with a mortar and pestle and stored at −80°C for further use.

Expression and purification of full length His_6::LET-99 were performed as described in (Wu and Rose, 2007), using Ni^{2+}-NTA agarose (Qiagen, Chatsworth, CA) and the manufacturer's protocol. To test if LET-99 interacts with PAR-5, 20 μg of bacterially expressed His6::LET-99 was added to 1 mg of embryo extract and incubated at 4°C overnight with or without 3mM ATP. The extracts were then re-purified on Ni^{2+}-NTA agarose beads, and the eluted samples subjected to SDS-PAGE and Western blotting with anti-LET-99 (1:4000), anti-tubulin (DM1a 1:10000), and anti-human 14-3-3 (H-8, Santa Cruz Biotechnology), which cross reacts with *C. elegans* PAR-5 (Lacoste et al., 2006).

Yeast two-hybrid analysis

Full length *par-5* (yk1741f.01, from Y. Kohara, National Institute of Genetics, Japan) and *let-99* (Tsou et al., 2002) cDNAs were separately subcloned into pGBD::TRP (containing GAL4 DNA binding domain (BD)) and pGAD::LEU2 (containing GAL4 activation domain (AD)). Pairwise combinations of AD and BD vectors were transformed sequentially into the yeast strain PJ69-4A and re-tested for the ability to grow on SD media lacking leucine, tryptophan and histidine (James et al., 1996). pGBD-PAR-5 alone activated expression of reporter genes (data not shown), and therefore all the yeast two hybrid interaction experiments were performed with pGAD-PAR-5 and pGBD-LET-99 variants. Standard molecular cloning methods and site-directed mutagenesis were used to create pGBD::LET-99 variants. To compare the interaction between different pGBD-LET-99 variants and pGAD-PAR-5, various pairwise yeast transformants were separately grown in liquid SD culture medium lacking leucine and tryptophan until they reached OD600=0.5. Two 10-fold serial dilutions for each culture were made, and 5μl of each were spotted onto SD plates lacking leucine, tryptophan and histidine; plates were incubated for 2 days at 30°C and then assessed for growth. All cultures and dilutions were tested in parallel on SD plates lacking only leucine and tryptophan to confirm growth of the co-transformants. Expression of each construct in yeast was confirmed by Western blots of yeast protein extracts probed with rabbit-anti-GAL4-BD (Abcam, ab24585; data not shown).

Generation of Transgenics

For bombardment, a 6.8kb rescuing fragment containing *let-99* genomic DNA with 1.9 kb upstream and 1.2 kb downstream of the *let-99* coding region (Tsou et al., 2002) was modified to encode an HA tag at the N-terminus; the *unc-119+* cassette was incorporated elsewhere in the plasmid. Site-directed mutagenesis (Quikchange, Agilent) was used to generate point mutations to change codons S124 and S248 to Alanine. Constructs were introduced into the DP38 *unc-119* using the microparticle bombardment method (Praitis et al., 2001). For MosSCI, the *let-99* genomic regions of the constructs above were subcloned into pCFJ151. Plasmids were injected with a source of transposase and co-injection markers into EG6699 as described in (Frokjaer-Jensen et al., 2014). Some bombardments and MosSCI were carried out by Knudra, Inc. Three HA::LET-99 lines generated by bombardment were identified but silenced over time. A single MosSCI HA::LET-99 line was obtained in which all early embryos showed cortical HA::LET-99 localization. This line was

crossed to *unc-119; unc-22 let-99(dd17)/ nT1* to generate worms homozygous for both *unc-22 let-99(dd17)* and the transgene (strain RL269). Multiple lines expressing HA::LET-99(2S>A) line were generated by bombardment, but only one line exhibited cortical signal in a significant number of early embryos. Three HA::LET-99(2S>A) lines were generated via MosSCI but exhibited cortical enrichment in less than 50% of embryos. The strongest staining lines from each method were crossed to *unc-22 let-99(dd17)/ DnT1* to generate worms homozygous for both *unc-22 let-99(dd17)* and the transgene (strains RL193 and RL307 respectively). RL193 embryos exhibited stronger cortical signal than RL307, and thus RL193 was used for quantitative analyses of staining patterns.

Immunofluorescence and quantification of staining intensities

Slides were prepared for in situ immunolocalization using standard freeze-crack and methanol fixation protocols as described (Miller and Shakes, 1995; Tsou et al., 2002). The following purified antibodies were used, each diluted in PBS with 3% bovine sheep albumin (BSA): chicken-anti-PAR-3 (1:40, Etemad-Moghadam et al., 1995), rabbit-anti-LET-99 (1:40, (Tsou et al., 2002), anti-mouse-HA (1:25, Abcam 12CA5), as well as rabbit-anti-PAR-1 antisera (1:1000; (Etemad-Moghadam et al., 1995; Guo and Kemphues, 1995). The following secondary antibodies were diluted in PBS with 3% BSA: FITC-goat-anti-rabbit (1:100, Jackson), rhodamine goat-anti-chicken (1:100, Sigma), Alexa-fluor-594 -donkey-anti-mouse (1:100, Jackson). Anti-PAR-3 and anti-LET-99 were pre-absorbed with acetone powder made from GST-expressing bacteria and secondary antibodies were pre-absorbed with acetone powder from wild-type worms. DAPI (4′,6-diamidino-2-phenylindole dihydrochloride) was used to label nuclei for determination of cell cycle stages.

For data reported in Fig. 1, single section (0.215μm) confocal images were taken at the mid-focal plane of the embryo with an Olympus FV1000 confocal microscope Fv1000 Fluoview Laser Scanning Confocal Microscope, using a 60x Plan-Apo NA 1.42 objective, using the same laser power and non-saturating exposure settings for all specimens. For quantification, intensity traces for a 0.4 μm -thick line drawn along the cortex from anterior to posterior tips were obtained using ImageJ (http://rsb.info.nih.gov/ij/). For quantification of embryos expressing HA-transgenes in Fig. 3, 10 z-slices at 0.15μm steps at a midfocal plane were acquired for both anti-HA and PAR-1 staining using the same microscope, and cortical intensities were measured as above in ImageJ using a maximum intensity projection; measurements were normalized to the average cytoplasmic intensity. Pixel values or normalized intensities were expressed as % embryo length (%EL), and traces were smoothened using a running average of 30, averaged by genotype and plotted using Prism (GraphPad). To compare transgene expression levels, measurements of whole cell staining intensity were made in ImageJ from maximum intensity projections using the freehand shape tool to trace around the entire embryo; for this analysis only embryos that were images with the same laser and exposure settings were used, and both embryos that did not show any cortical enrichment were also included.

Live imaging of early embryos

Embryos were cut from gravid hermaphrodites in egg buffer, mounted on polylysine coated coverslips and inverted over spacers for imaging with DIC optics using an Olympus BX60

microscope with PlanApo N 60X, 1.42 NA objective lens. All embryos were filmed at a room temperature of 23-25°C, with the exception of *let-99(ax218ts)* embryos, which were filmed at 17-20°C using a Linkam PE95/T95 System Controller with ECP Water Circulation Pump. Images were captured at five-second intervals using a Hammatasu Orca 12-bit digital camera and OpenLab Software. Measurements were made on still images in Openlab using the ruler tool, or extracted from manual tracking data of centrosomes during the time-lapse (Manual Tracking plugin for ImageJ (rsbweb.nih.gov/ij/plugins/track/track.html). The distance in pixels from the anterior edge of the embryo (=0% EL) to each centrosome was determined at NEB and at the onset of cytokinesis. The midpoint between the centrosomes was calculated in excel, and divided by EL to determine the position of centration at NEB and the final spindle position at cytokinesis. The difference between these midpoints was used to calculate spindle displacement. The angle of rotation was measured in Openlab, using the angle between a line drawn through the centrosomes at NEB and a line drawn on the AP axis. Scatter plots and statistical analysis were carried out using PrismPlot (GraphPad Software, Inc). Unpaired, two-tailed Students t-tests were used to compare all data.

RESULTS AND DISCUSSION

Cortical LET-99 localization is abnormal in *par-5* mutants

Of the two *C. elegans* 14-3-3 genes, *par-5* is the only 14-3-3 required for oogenesis and early embryo development. Strong reduction in PAR-5 levels results in germ-line defects and sterility (Aristizabal-Corrales et al., 2012; Wang and Shakes, 1997). However defects in one-cell polarity can be observed in embryos derived from mothers with a partial loss of PAR-5 function generated by RNA interference (RNAi) or the use of maternal specific alleles (Morton et al., 2002). In such embryos, the PAR-3 and PAR-2 domains show extensive overlap with one another. Similarly, PAR-1 expands to occupy more anterior regions of the cortex but is still present at the very posterior pole of the embryo. Thus, even though PAR-5 exhibits symmetric cortical and cytoplasmic localization, it is nonetheless required for defining the anterior/posterior PAR polarity domain boundaries (Morton et al., 2002)(Fig. 1).

Our previous work suggested that LET-99 is inhibited by gradients of PAR proteins at the cortex (Wu and Rose, 2007). Thus, we first quantified PAR-3 and PAR-1 immunostaining in *par-5(RNAi)* embryos compared to wild type (Fig. 1A, B). The pixel intensities of a line drawn on the cortex from the anterior pole to the posterior pole were measured and plotted as a function of total embryo length (%EL,). Quantification was carried out on late prophase to metaphase stages, because in anaphase *par-5(RNAi)* embryos, PAR-3 expanded even further into the posterior (n=9), consistent with previous studies (Etemad-Moghadam et al., 1995; Mikl and Cowan, 2014). In *par-5(RNAi)* embryos, PAR-3 levels were similar to those observed in wild-type embryos at the very anterior, but the PAR-3 gradient was shallower and extended more posteriorly (Fig. 1B, n= 12 wild type and 8 *par-5*). As expected, the domain with high levels of PAR-1 was smaller in *par-5* embryos compared to wild type. Nonetheless, the peak levels of PAR-1 at the posterior were similar to those seen in wild type (Fig. 1B).

We next examined the localization pattern of LET-99. If PAR-3 and/or PAR-1 normally utilize PAR-5 as a mediator to inhibit LET-99 cortical localization, then in *par-5(RNAi)* embryos LET-99 should localize to areas with high levels of PAR-3 and/or PAR-1 (Fig. 1C). In wild-type embryos, cortical LET-99 localization was highest in a posterior-lateral band present from approximately 55-75%EL (n= 20, Fig. 1D,E) as previously published. Interestingly, we found that in *par-5(RNAi)* embryos, the highest levels of LET-99 localization were at the very posterior cortex rather than in a band pattern (Fig. 1D,E). In *par-5(RNAi)* embryos, cortical LET-99 levels started to elevate from ~80%EL, comparable to the region where high levels of PAR-1 are present at the cortex in *par-5* mutant embryos (compare Fig. 1, B and E). In contrast, high levels of LET-99 did not overlap with the anterior domain occupied by PAR-3 in *par-5(RNAi)* embryos (n=7).

The lower levels of LET-99 at the anterior cortex suggest that cortical LET-99 localization is still inhibited by the anterior PAR-3/PAR-6/PKC-3 complex in the absence of PAR-5. Conversely, the overlap between PAR-1 and LET-99 is consistent with the model that PAR-5 is required for PAR-1's ability to inhibit LET-99 localization at the posterior cortex (Fig. 1C).

LET-99 interacts with PAR-5 through predicted 14-3-3 binding sites

To test if the 14-3-3 protein PAR-5 interacts with LET-99, we incubated bacterially expressed His::LET-99 with wild-type embryo extracts in the presence or absence of physiological concentrations of ATP. PAR-5 co-purified with His::LET-99 in the presence of excess ATP (Fig. 2A). PAR-1 also co-purified with His::LET-99 as previously shown (Wu and Rose, 2007) and this interaction did not appear to depend on the addition of excess ATP.

Three classes of binding motifs, all of which contain a potential phosphorylation site, have been identified in target proteins that interact with 14-3-3 proteins (Obsil and Obsilova, 2011). Using the ELM Linear Motif prediction tool (Puntervoll et al., 2003), five potential 14-3-3 binding sites were predicted in LET-99 (Fig. 2B). To test the relevance of the predicted sites, we tested for interactions between LET-99 and PAR-5 using the yeast two-hybrid assay (Fig. 2B). Even though phosphorylation of the target protein is typically required for binding to 14-3-3 proteins, interactions have been observed in this assay, presumably because the target is phosphorylated by a yeast kinase (Benton et al., 2002; Benton and St Johnston, 2003; Popovici et al., 2006). We first tested full-length wild-type LET-99 as well as several regions of LET-99 for interaction with full-length PAR-5. Full-length LET-99 interacted strongly with PAR-5, as did the N-terminal 293 amino acids, which contains the DEP domain. However, the DEP domain alone was not sufficient for interaction with PAR-5 in this assay, and a version of LET-99 deleted for the DEP domain was able to interact with PAR-5. We therefore focused on the three potential PAR-5 binding sites present in the 1-293 fragment.

The predicted serine or threonine phosphorylation sites in the PAR-5 binding motifs were mutated to alanine either individually or in combination in the LET-99 (1-293) fragment and tested in the yeast two-hybrid assay. When either serine residue 124 or 248, but not threonine residue 272, was mutated to alanine, LET-99 (1-293) showed reduced interaction with PAR-5. Mutation of both S124 and S248 in either LET-99 (1-293) or full-length

LET-99 abolished interaction with PAR-5. We conclude that serines 124 and 248 of LET-99 are required for LET-99 association with PAR-5 in this assay.

14-3-3-binding sites are needed for normal localization of LET-99 in early embryos

To test whether the PAR-5 binding sites identified are relevant *in vivo*, we generated transgenic animals expressing LET-99 that contained either wild-type or mutant binding sites. We previously demonstrated that a genomic fragment of *let-99* driven by its endogenous promoter rescues *let-99* maternal effect lethality and spindle positioning phenotypes (Tsou et al., 2002). We generated a parallel transgene with an N-terminal hemagluttin (HA) epitope, HA::LET-99, as well as a transgene with the HA tag and serine-to-alanine mutations at residues 124 and 248, HA::LET-99(2S>A). Lines with integrated transgenes were generated using biolistic particle bombardment and Mos1-mediated single copy insertion (MosSCI)(Frokjaer-Jensen et al., 2014; Praitis et al., 2001). Worms containing the transgene were then crossed to a *let-99(null)* balanced strain to generate worms homozygous for *let-99* and the transgene (see methods). One HA::LET-99 transgenic line (RL269) and two HA::LET-99(2S>A) lines (RL193 and RL307) were analyzed further by immunostaining with anti-HA antibodies and PAR-1 antibodies.

All one-cell embryos from the RL269 strain exhibited HA::LET-99 at the cortex in prometaphase through anaphase stage one-cell embryos, as previously reported for endogenous LET-99 (Tsou et al., 2002; Wu and Rose, 2007). In contrast, weak cortical enrichment of HA::LET-99(2S>A) was observed in only 23/33 one-cell RL193 embryos at the same stages. To compare the patterns of HA::LET-99 and HA::LET-99 (2S>A), we quantified the level of cortical enrichment by measuring cortical pixel intensities along the anterior-posterior axis, normalized to cytoplasmic pixel intensities. Prometaphase through metaphase embryos were first examined, because LET-99 localization in wild-type embryos is PAR-dependent during these stages (Bringmann et al., 2007; Tsou et al., 2002; Wu and Rose, 2007). As expected, HA::LET-99 localized in a posterior-lateral band at the cortex, with highest levels from approximately 55-75% EL on average (n= 10, Fig. 3). In the subset of prometaphase to metaphase stage RL193 one-cell embryos that showed some cortical enrichment, (HA::LET-99(2S>A) staining was present in a weak anterior to posterior gradient, with the highest enrichment at the posterior pole (n=13, Fig. 3). Thus, the highest levels of HA::LET-99(2S>A) overlapped with PAR-1 in these embryos. Similarly, of the 3/8 RL307 one-cell embryos that showed an enrichment of HA::LET-99(2S>A) at the cortex, all 3 had higher levels at the posterior.

Interestingly, in the anaphase RL193 embryos that showed cortical enrichment, 8/10 embryos had a banded pattern while 2/10 still exhibited posterior enrichment (compared to 8/8 embryos with a band in RL269 worms). These results are consistent with previous work showing that a band of LET-99 can form late in anaphase in *par-3* and *par-1* mutant embryos and that the spindle can influence LET-99 localization at this time (Bringmann et al., 2007; Tsou et al., 2002; Wu and Rose, 2007).

In wild-type embryos at the two-cell stage, PAR domains are reestablished in the P1 daughter (Rose and Gonczy, 2014). LET-99 becomes localized in a banded pattern by prophase in the P1 cell, in a PAR-1 dependent manner (Tsou et al., 2002; Wu and Rose,

2007). We could not directly test the requirements for PAR-5 in localizing LET-99 in this cell, because the P1 cell doesn't repolarize in *par-5(RNAi)* two-cell embryos (Morton et al., 2002). However, we observed that HA::LET-99(2S>A) was present at highest levels in the posterior at prophase and metaphase in the P1 cell of RL193 two-cell embryos, just as in the one-cell (n=5; Fig. 3).

Overall these results demonstrate that the predicted PAR-5/14-3-3 binding sites identified in the yeast two-hybrid assay are required for the normal pattern of LET-99 localization in the one-cell embryo and in the P1 cell. The presence of the highest levels of cortical HA::LET-99(2S>A) at the very posterior pole is consistent with a model in which binding of PAR-5 acts downstream of PAR-1 to inhibit cortical localization to the posterior cortex. In this model, loss of interaction with PAR-5 is also predicted to allow accumulation of higher levels of LET-99 at the cortex, as we previously observed for LET-99 localization in *par-1* embryos (Wu and Rose, 2007). In contrast, we observed significantly lower cortical enrichment of the HA::LET-99(2S>A) protein compared to the HA::LET-99 protein (Fig. 3B,D) even when the domains with the highest cortical enrichment for each genotype were compared (1.2 for 80-100%EL in RL193 versus 1.6 for 55-75%EL in RL269, $p = 0.006$). This difference in cortical signal is not due to lower transgene expression in the HA::LET-99(2S>A) lines. The whole-cell staining intensities of one-cell embryos from RL269 embryos (mean 2159.32, standard deviation 456.32) were not statistically different than those of RL193 (2379.91, 454.04; $p=0.38$) and RL307 (2371.44, 570.90, $p=0.47$). Thus, the S124A and S248A mutations affect not only the asymmetry of LET-99, but its cortical accumulation.

HA::LET-99(2S>A) expression partially rescues the *let-99* phenotype

We next used DIC time-lapse video microscopy to examine early embryos from the transgenic strains compared to wild-type and mutant controls, and quantified several aspects of nuclear-centrosome and spindle movements (Fig. 4; (Galli and van den Heuvel, 2008; Rose and Gonczy, 2014)). In wild-type one-cell embryos during prophase, the female and male pronuclei meet at the posterior end, and then the nuclear-centrosome complex moves anteriorly in a process called centration (Fig. 4A,B; Movie 1). The entire complex also rotates such that the angle of the centrosomes is usually within 30° of the AP axis prior to nuclear envelope breakdown (NEB) and spindle formation, although greater angles are observed in some embryos (Fig. 4A, C). During metaphase/anaphase, the spindle is displaced towards the posterior (Fig. 4A, D). Rotation of the nuclear-centrosome complex onto the AP axis occurs again in the P1 cell at the two-cell stage, while the spindle in the AB cell sets up at a 90° angle to the AP axis (Fig. 4A, E). Embryos from *let-99(null)* mutant mothers (hereafter *let-99* embryos) display vigorous rocking movements of the nuclear-centrosome complex instead of the normal smooth centration and rotation movements, resulting in variable centration and rotation positions compared to wild type (n=13, Fig. 4B,C; Movie 2; (Rose and Kemphues, 1998; Tsou et al., 2002). In both wild type and *let-99* embryos, when nuclear rotation is incomplete before NEB, the spindle nonetheless aligns with the AP axis during metaphase/anaphase; this is due to cell shape constraints (Tsou et al., 2002; Tsou et al., 2003b). In *let-99* embryos, the spindle midpoint doesn't move further posterior during anaphase (Fig. 4D); however, the final spindle position is similar to wild

type and produces an uequal division, because of failed centration (Rose and Kemphues, 1998; Tsou et al., 2002). In two-cell *let-99* embryos, the P1 nucleus fails to rotate by NEB in most embryos (Fig. 4E) and remains misoriented.

Embryos from RL269, expressing wild-type HA::LET-99, exhibited smooth anteriorly-directed centration and rotation movements, without nuclear centrosome rocking, similar to wild type (n=10, Movie 3; Fig. 4B,C). The extent of spindle displacement was also more similar to wild-type than to *let-99* embryos, and the P1 spindle rotated at the two-cell stage (Fig. 4D,E) Thus, HA-tagged LET-99 rescued the *let-99(null)* mutant phenotype. In contrast, embryos from RL193 expressing HA::LET-99(2S>A) exhibited a moderate nuclear rocking phenotype in one-cell embryos (n=11). Many of these embryos also exhibited defects in centration, rotation and spindle displacement that were similar to *let-99(null)* mutants, although not as severe (Movie 4, Fig. 4B-F). At the two-cell stage, P1 nuclear rotation often did not occur by NEB in most RL193 embryos (9/11; Fig. 4E), however the spindle shifted late in division to become more aligned on the AP axis in four of these embryos. These and the embryos that underwent nuclear rotation with normal timing exhibited a normal cellular arrangement and division pattern at third cleavage, which correlates with the rescue of lethality in this line. Embryos from the RL307 HA::LET-99(2S>A) line exhibited similar phenotypes (Fig. 4). Thus, the S>A transgene can partially rescue *let-99* nuclear and spindle movement phenotypes, but not to the same extent as the HA::LET-99 transgene.

We had predicted that the presence of HA::LET-99(2S>A) at the posterior pole would fully rescue *let-99's* defects in centration and rotation, based on studies of *par-1*. In *par-1* embryos, the position of centration and nuclear rotation are normal in the one cell and in the P1 cell (Kemphues et al., 1988; Wu and Rose, 2007). The higher level of LET-99 at the entire posterior cortex compared to the anterior cortex (rather than a band) in this background is thought to inhibit pulling forces at the posterior, allowing for centration and rotation. In addition redundant mechanisms, including cell shape, affect centration/rotation, and our previous work showed that rotation is less robust in *par-1* mutants when cell shape is perturbed (Kimura and Kimura, 2011; Tsou et al., 2003b; Wu and Rose, 2007). Overall, the abnormal phenotypes of *let-99*; HA::LET-99 (2S>A) embryos are not similar to *par-1* embryos, but rather suggest a partial loss of *let-99* function. To test this, we examined a *let-99(ts*) allele at intermediate temperature. These *let-99(ts*) embryos showed abnormal nuclear rocking (n=11), partial centration and rotation defects, and defective spindle displacement (Movie 5, Fig. 4). At the two-cell stage, P1 rotation did not occur before NEB in most embryos, but late rotations occurred producing a normal four-cell arrangement (14/19). Thus, the phenotypes of *let-99(ts)* and RL193 *let-99*; HA::LET-99 (2S>A) are very similar.

A key difference between LET-99 localization in HA::LET-99(2S>A) embryos and *par-1* mutant embryos is the lower cortical enrichment of HA::LET-99(2S>A). Our previous studies showed that *par-1* embryos had higher cortical enrichments at the posterior than in the band of wild-type embryos (Wu and Rose, 2007) whereas here cortical enrichment of HA::LET-99(2S>A) embryos was lower than in wild type, and some embryos showed no apparent enrichment. Thus, the intermediate *let-99* phenotypes observed in HA::LET-99(2S>A) embryos are likely due to lower cortical levels of LET-99, rather than

mislocalization to the posterior pole of the embryo. As mentioned, the whole cell staining intensities for RL193 and RL307 were not lower than for RL269. Thus, together these observations suggest that the S>A mutations also impair the cortical localization of LET-99. One possibility is that the region of LET-99 that associates with PAR-5 also associates with a cortical or membrane anchor for LET-99.

CONCLUDING REMARKS

Using a combination of PAR-5 depletion, *in vitro* biochemistry, and *in vivo* immunolocalization of wild-type and mutated LET-99, we showed that PAR-5 restricts LET-99 from the posterior cortex. However, PAR-5 is not required for the inhibition of LET-99 from the anterior PAR domain. PAR-5 is itself uniformly localized in the cytoplasm and at the cortex (Morton et al., 2002;(Etemad-Moghadam et al., 1995; Mikl and Cowan, 2014). Thus, these observations suggest that distinct mechanisms regulate the cortical inhibition of LET-99 at the anterior versus the posterior poles. Because 14-3-3 protein typically bind phosphorylated targets (reviewed in (Aristizabal-Corrales et al., 2012; Gardino and Yaffe, 2011; Obsil and Obsilova, 2011), the results reported here and in previous studies (Wu and Rose, 2007) support a model in which LET-99 is phosphorylated on 14-3-3 sites in the posterior by PAR-1 or a kinase downstream of PAR-1. Phosphorylated LET-99 then associates with PAR-5, which prevents LET-99's accumulation at the posterior-most cortex.

Prior to this study, a genetic requirement for 14-3-3 proteins in regulating the cortical asymmetric localization of the PAR polarity proteins was shown in *C. elegans* one-cell embryos and several other polarized cell types. Mechanistic studies in both *Drosophila* and mammalian epithelial cells showed that PKC-3 phosphorylates PAR-1 and PAR-1 phosphorylates PAR-3 on 14-3-3 sites; subsequent association with PAR-5 orthologs prevents overlap of PAR domains (Benton and St Johnston, 2003; Goransson et al., 2006; Suzuki et al., 2004). However, few other studies have reported a role for PAR-5 in facilitating the regulation of targets downstream of the PAR polarity proteins. One clear example is the asymmetric cortical localization of LGN (a GPR ortholog), a component of the force-generating complex in cultured MDCK cell cysts. Phosphorylation of LGN by atypical PKC (PKC-3) prevents LGN localization to the apical cortex, thus restricting it to cell-cell contacts and ensuring symmetric division and maintenance of the cyst lumen (Hao et al., 2010). A requirement for 14-3-3 binding sites has also been demonstrated for Exuperentia, a target of PAR-1 in Drosophila oocyte asymmetry; however, direct binding of the PAR-5/14-3-3 protein to Exuperentia was not examined (Riechmann and Ephrussi, 2004). 14-3-3 proteins are known to coordinately regulate multiple proteins involved in a given process, such as cell proliferation or apoptosis (Aristizabal-Corrales et al., 2012; Gardino and Yaffe, 2011). Thus, given our work on LET-99 and the two cases cited above, it will be interesting to determine if PAR-1 and PKC-3 regulate other downstream targets in asymmetric division via 14-3-3 interactions.

14-3-3 proteins regulate the localization or activity of diverse substrates in many different cell types (reviewed in (Freeman and Morrison, 2011; Gardino and Yaffe, 2011; Obsil and Obsilova, 2011). Some 14-3-3 family members alter protein levels by promoting the stability

of their substrates while in other cases interaction with 14-3-3 proteins promotes degradation. Degradation of LET-99 in the posterior via PAR-5 interaction would seem unlikely to promote spatial regulation of LET-99 unless degradation is highly localized near the membrane, because cytoplasmic LET-99 appears uniform along the AP axis in the one-cell embryo (Fig. 1)(Wu and Rose, 2007). Further, quantification of whole cell staining intensities did not reveal significantly higher levels of HA::LET-99(2S>A) compared to HA::LET-99 (this study), or in *par-1* embryos compared to wild-type (Wu and Rose, 2007). Many 14-3-3 proteins lock their substrates in a certain conformation that affects their activity or their association with other binding partners. Similarly, 14-3-3 proteins can change a target protein's localization by masking targeting signals. Thus, we propose that PAR-5 affects LET-99's cortical asymmetry by changing LET-99's ability to interact with lipids or protein anchors at the plasma membrane. Future studies will determine the mechanism by which LET-99 associates with the cortex/plasma membrane and how PAR-5 affects this association, as well as why PAR-5 only regulates the posterior localization of LET-99.

Supplementary Material

Refer to Web version on PubMed Central for supplementary material.

ACKNOWLDEGMENTS

We thank Adam Hayashi and Meng-fu Bryan Tsou for help with plasmid constructs and transgene generation, and Jennifer Milan and Malgorzata Liro for help with embryo filming. We are grateful to the Nunnari and Shiozaki labs for advice on yeast assays, Ken Kemphues (Cornell University) for sharing antibodies, and Geraldine Seydoux (Johns Hopkins University) for the original *ax218* strains. Members of the Rose and McNally lab provided helpful discussion. This work was supported by NIH 1R01GM68744 to L. R., part of which was funded by the ARRA, and by NIFA CA-D* -MCB-6239-H. E. E. also received funding from the Floyd and Mary Schwall Fellowship in Medical Research, the Floyd and Mary Schwall Dissertation Year Fellowship and an NIH Molecular and Cellular Biology Training Grant T32GM007377.

REFERENCES

Aristizabal-Corrales D, Schwartz S Jr. Ceron J. PAR-5 is a PARty hub in the germline: Multitask proteins development and disease. Worm 1. 2013; 2(1):e21834.

Aristizabal-Corrales D, Fontrodona L, Porta-de-la-Riva M, Guerra-Moreno A, Ceron J, Schwartz S Jr. The 14-3-3 gene par-5 is required for germline development and DNA damage response in Caenorhabditis elegans. Journal of cell science. 2012; 125:1716–1726. [PubMed: 22328524]

Benton R, Palacios IM, St Johnston D. Drosophila 14-3-3/PAR-5 is an essential mediator of PAR-1 function in axis formation. Developmental cell. 2002; 3:659–671. [PubMed: 12431373]

Benton R, St Johnston D. Drosophila PAR-1 and 14-3-3 inhibit Bazooka/PAR-3 to establish complementary cortical domains in polarized cells. Cell. 2003; 115:691–704. [PubMed: 14675534]

Brenner S. The genetics of Caenorhabditis elegans. Genetics. 1974; 77:71–94. [PubMed: 4366476]

Bringmann H, Cowan CR, Kong J, Hyman AA. LET-99, GOA-1/GPA-16, and GPR-1/2 are required for aster-positioned cytokinesis. Curr Biol. 2007; 17:185–191. [PubMed: 17189697]

Church DL, Guan KL, Lambie EJ. Three genes of the MAP kinase cascade, mek-2, mpk-1/sur-1 and let-60 ras, are required for meiotic cell cycle progression in Caenorhabditis elegans. Development. 1995; 121:2525–2535. [PubMed: 7671816]

Etemad-Moghadam B, Guo S, Kemphues KJ. Asymmetrically distributed PAR-3 protein contributes to cell polarity and spindle alignment in early C. elegans embryos. Cell. 1995; 83:743–752. [PubMed: 8521491]

Florian MC, Geiger H. Concise review: polarity in stem cells, disease, and aging. Stem cells. 2010; 28:1623–1629. [PubMed: 20641041]

Freeman AK, Morrison DK. 14-3-3 Proteins: diverse functions in cell proliferation and cancer progression. Seminars in cell & developmental biology. 2011; 22:681–687. [PubMed: 21884813]

Frokjaer-Jensen C, Davis MW, Sarov M, Taylor J, Flibotte S, LaBella M, Pozniakovsky A, Moerman DG, Jorgensen EM. Random and targeted transgene insertion in Caenorhabditis elegans using a modified Mos1 transposon. Nature methods. 2014; 11:529–534. [PubMed: 24820376]

Galli M, Munoz J, Portegijs V, Boxem M, Grill SW, Heck AJ, van den Heuvel S. aPKC phosphorylates NuMA-related LIN-5 to position the mitotic spindle during asymmetric division. Nature cell biology. 2011; 13:1132–1138. [PubMed: 21857670]

Galli M, van den Heuvel S. Determination of the cleavage plane in early C. elegans embryos. Annu Rev Genet. 2008; 42:389–411. [PubMed: 18710303]

Gardino AK, Yaffe MB. 14-3-3 proteins as signaling integration points for cell cycle control and apoptosis. Seminars in cell & developmental biology. 2011; 22:688–695. [PubMed: 21945648]

Gonczy P. Mechanisms of asymmetric cell division: flies and worms pave the way. Nature reviews. Molecular cell biology. 2008; 9:355–366. [PubMed: 18431399]

Goransson O, Deak M, Wullschleger S, Morrice NA, Prescott AR, Alessi DR. Regulation of the polarity kinases PAR-1/MARK by 14-3-3 interaction and phosphorylation. Journal of cell science. 2006; 119:4059–4070. [PubMed: 16968750]

Guo S, Kemphues KJ. par-1, a gene required for establishing polarity in C. elegans embryos, encodes a putative Ser/Thr kinase that is asymmetrically distributed. Cell. 1995; 81:611–620. [PubMed: 7758115]

Hao Y, Du Q, Chen X, Zheng Z, Balsbaugh JL, Maitra S, Shabanowitz J, Hunt DF, Macara IG. Par3 controls epithelial spindle orientation by aPKC-mediated phosphorylation of apical Pins. Curr Biol. 2010; 20:1809–1818. [PubMed: 20933426]

James P, Halladay J, Craig EA. Genomic libraries and a host strain designed for highly efficient two-hybrid selection in yeast. Genetics. 1996; 144:1425–1436. [PubMed: 8978031]

Kamath RS, Fraser AG, Dong Y, Poulin G, Durbin R, Gotta M, Kanapin A, Le Bot N, Moreno S, Sohrmann M, Welchman DP, Zipperlen P, Ahringer J. Systematic functional analysis of the Caenorhabditis elegans genome using RNAi. Nature. 2003; 421:231–237. [PubMed: 12529635]

Kemphues KJ, Priess JR, Morton DG, Cheng NS. Identification of genes required for cytoplasmic localization in early C. elegans embryos. Cell. 1988; 52:311–320. [PubMed: 3345562]

Kimura K, Kimura A. Intracellular organelles mediate cytoplasmic pulling force for centrosome centration in the Caenorhabditis elegans early embryo. Proc Natl Acad Sci U S A. 2011; 108:137–142. [PubMed: 21173218]

Kiyomitsu T. Mechanisms of daughter cell-size control during cell division. Trends in cell biology. 2014

Knoblich JA. Asymmetric cell division: recent developments and their implications for tumour biology. Nature reviews. Molecular cell biology. 2010; 11:849–860. [PubMed: 21102610]

Kotak S, Gonczy P. Mechanisms of spindle positioning: cortical force generators in the limelight. Current opinion in cell biology. 2013; 25:741–748. [PubMed: 23958212]

Krueger LE, Wu JC, Tsou MF, Rose LS. LET-99 inhibits lateral posterior pulling forces during asymmetric spindle elongation in C. elegans embryos. J Cell Biol. 2010; 189:481–495. [PubMed: 20421425]

Lacoste C, Barthaux V, Iborra C, Seagar M, Erard-Garcia M. MAU-8 is a Phosducin- like Protein required for G protein signaling in C. elegans. Developmental biology. 2006; 294:181–191. [PubMed: 16580661]

Lewis JA, Fleming JT. Basic culture methods. Methods in cell biology. 1995; 48:3–29. [PubMed: 8531730]

Mikl M, Cowan CR. Alternative 3' UTR selection controls PAR-5 homeostasis and cell polarity in C. elegans embryos. Cell reports. 2014; 8:1380–1390. [PubMed: 25199833]

Miller DM, Shakes DC. Immunofluorescence microscopy. Methods in cell biology. 1995; 48:365–394. [PubMed: 8531735]

Morin X, Bellaiche Y. Mitotic spindle orientation in asymmetric and symmetric cell divisions during animal development. Dev Cell. 2011; 21:102–119. [PubMed: 21763612]

Morton DG, Shakes DC, Nugent S, Dichoso D, Wang W, Golden A, Kemphues KJ. The Caenorhabditis elegans par-5 gene encodes a 14-3-3 protein required for cellular asymmetry in the early embryo. Developmental biology. 2002; 241:47–58. [PubMed: 11784094]

Nance J, Zallen JA. Elaborating polarity: PAR proteins and the cytoskeleton. Development. 2011; 138:799–809. [PubMed: 21303844]

Obsil T, Obsilova V. Structural basis of 14-3-3 protein functions. Seminars in cell & developmental biology. 2011; 22:663–672. [PubMed: 21920446]

Park DH, Rose LS. Dynamic localization of LIN-5 and GPR-1/2 to cortical force generation domains during spindle positioning. Developmental biology. 2008; 315:42–54. [PubMed: 18234174]

Popovici C, Berda Y, Conchonaud F, Harbis A, Birnbaum D, Roubin R. Direct and heterologous approaches to identify the LET-756/FGF interactome. BMC genomics. 2006; 7:105. [PubMed: 16672054]

Praitis V, Casey E, Collar D, Austin J. Creation of low-copy integrated transgenic lines in Caenorhabditis elegans. Genetics. 2001; 157:1217–1226. [PubMed: 11238406]

Puntervoll P, Linding R, Gemund C, Chabanis-Davidson S, Mattingsdal M, Cameron S, Martin DM, Ausiello G, Brannetti B, Costantini A, Ferre F, Maselli V, Via A, Cesareni G, Diella F, Superti-Furga G, Wyrwicz L, Ramu C, McGuigan C, Gudavalli R, Letunic I, Bork P, Rychlewski L, Kuster B, Helmer-Citterich M, Hunter WN, Aasland R, Gibson TJ. ELM server: A new resource for investigating short functional sites in modular eukaryotic proteins. Nucleic acids research. 2003; 31:3625–3630. [PubMed: 12824381]

Riechmann V, Ephrussi A. Par-1 regulates bicoid mRNA localisation by phosphorylating Exuperantia. Development. 2004; 131:5897–5907. [PubMed: 15539486]

Rose L, Gonczy P. Polarity establishment, asymmetric division and segregation of fate determinants in early C. elegans embryos. WormBook : the online review of C. elegans biology. 2014:1–43.

Rose LS, Kemphues K. The let-99 gene is required for proper spindle orientation during cleavage of the C. elegans embryo. Development. 1998; 125:1337–1346. [PubMed: 9477332]

Siller KH, Doe CQ. Spindle orientation during asymmetric cell division. Nature cell biology. 2009; 11:365–374. [PubMed: 19337318]

Suzuki A, Hirata M, Kamimura K, Maniwa R, Yamanaka T, Mizuno K, Kishikawa M, Hirose H, Amano Y, Izumi N, Miwa Y, Ohno S. aPKC acts upstream of PAR-1b in both the establishment and maintenance of mammalian epithelial polarity. Curr Biol. 2004; 14:1425–1435. [PubMed: 15324659]

Timmons L, Fire A. Specific interference by ingested dsRNA. Nature. 1998; 395:854. [PubMed: 9804418]

Tsou MF, Hayashi A, DeBella LR, McGrath G, Rose LS. LET-99 determines spindle position and is asymmetrically enriched in response to PAR polarity cues in C. elegans embryos. Development. 2002; 129:4469–4481. [PubMed: 12223405]

Tsou MF, Hayashi A, Rose LS. LET-99 opposes Galpha/GPR signaling to generate asymmetry for spindle positioning in response to PAR and MES-1/SRC-1 signaling. Development. 2003a; 130:5717–5730. Epub 2003 Oct 5718. [PubMed: 14534135]

Tsou MF, Ku W, Hayashi A, Rose LS. PAR-dependent and geometry-dependent mechanisms of spindle positioning. J Cell Biol. 2003b; 160:845–855. [PubMed: 12642612]

Wang W, Shakes DC. Expression patterns and transcript processing of ftt-1 and ftt-2, two C. elegans 14-3-3 homologues. Journal of molecular biology. 1997; 268:619–630. [PubMed: 9171285]

Williams SE, Fuchs E. Oriented divisions, fate decisions. Current opinion in cell biology. 2013; 25:749–758. [PubMed: 24021274]

Wu JC, Rose LS. PAR-3 and PAR-1 inhibit LET-99 localization to generate a cortical band important for spindle positioning in Caenorhabditis elegans embryos. Molecular biology of the cell. 2007; 18:4470–4482. [PubMed: 17761536]

Highlights

PAR-5 is required for cortical LET-99 asymmetry in embryos,

PAR-5 associates with LET-99 in pull down assays and in the yeast two-hybrid system.

Mutation of two predicted PAR-5 binding sites abolishes binding in yeast and alters LET-99 localization in vivo.

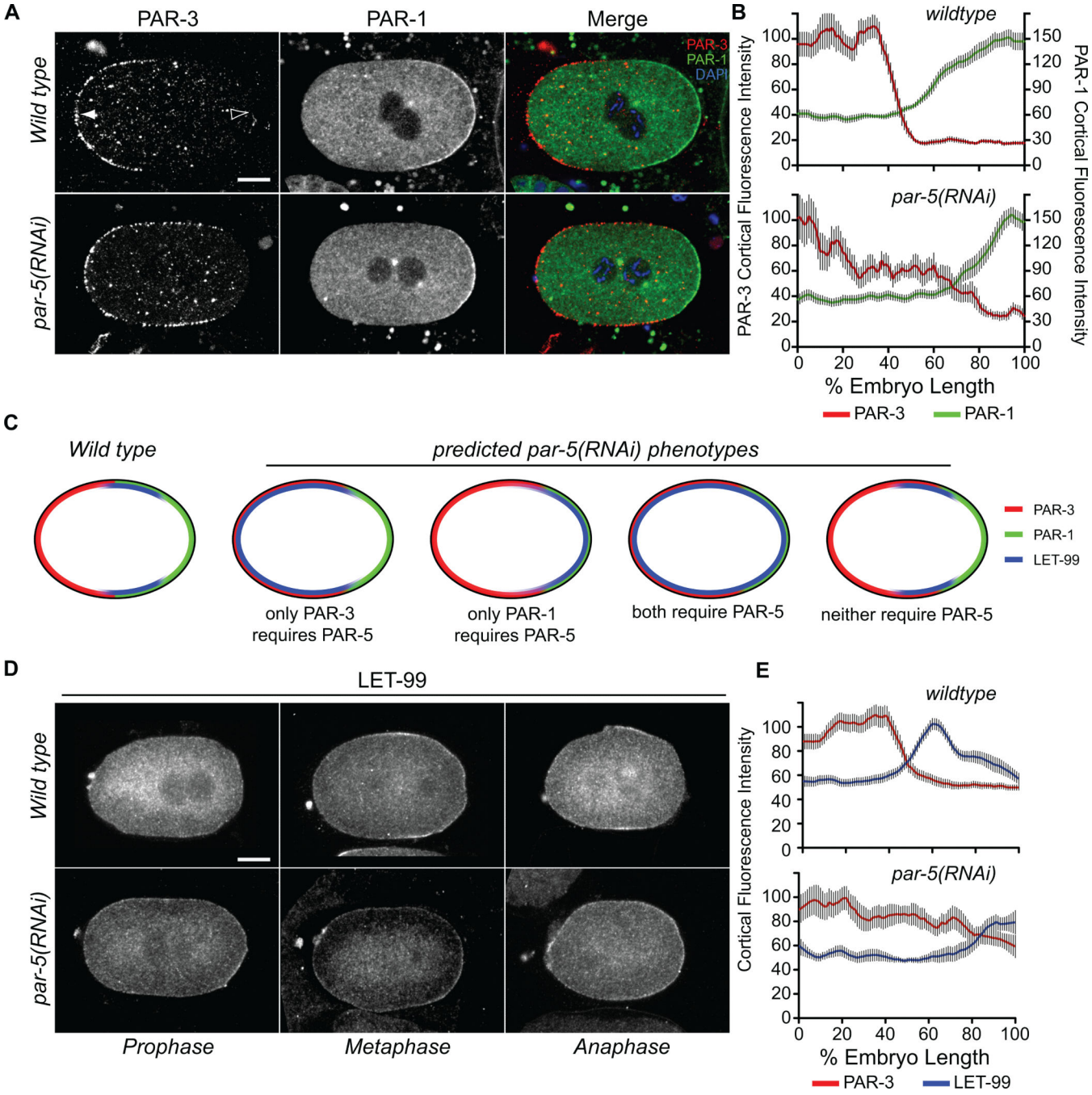

Fig. 1.

LET-99 localization is dependent on *par-5*. (A) Confocal images of wild-type and *par-5(RNAi)* prophase embryos, stained for PAR-3 and PAR-1. Arrowheads in first panel mark the beginning (0%EL, white,) and ending (100%EL, open white) positions of the cortical intensity traces. (B) Quantification of average cortical fluorescence staining intensities for PAR-3 and PAR-1; n= 12 wild type and 8 *par-5* embryos (C) Schematic diagrams of PAR and LET-99 domains in a wild-type embryo and in predictions for *par-5(RNAi)* embryos, based on whether the inhibition of LET-99 from cortical domains

depends on PAR-3 and PAR-1 as listed below the diagram. (D) Confocal images of representative wild-type and *par-5(RNAi)* embryos stained for LET-99. (B) Quantification of average cortical fluorescence staining intensities for embryos stained for both PAR-3 and LET-99 in wild type (n=20) and *par-5 (RNAi)* (n=7). Scale bars: 10 μm.

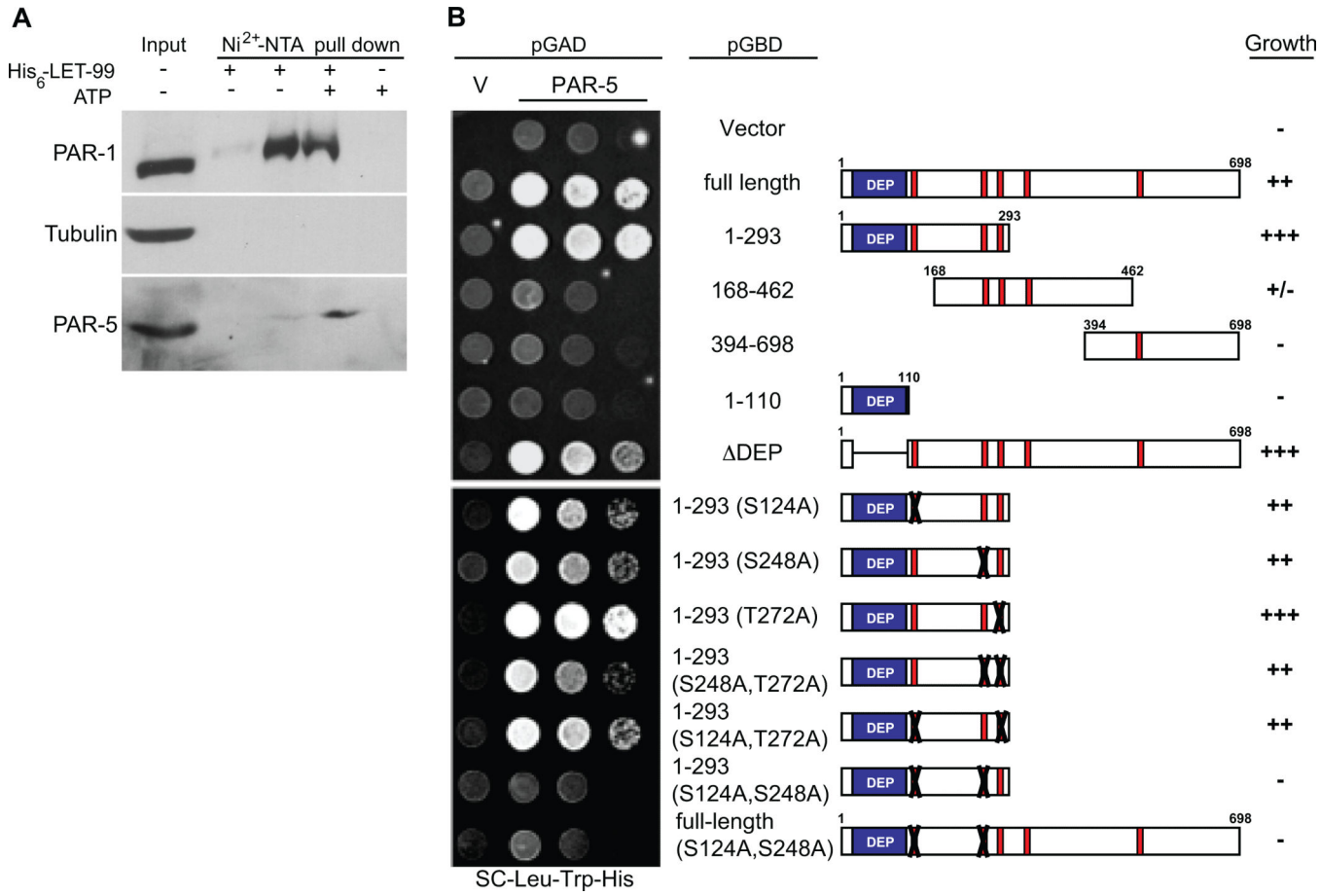

Fig. 2.

LET-99 interacts with PAR-5 through two 14-3-3 sites. A) His_6-LET-99 was incubated with wild-type embryo extract with or without added ATP and re-purified by Ni^{2+}-NTA chromatography. Western blots of the input and pull down products probed with anti-LET-99, anti-tubulin, and anti-PAR-5 antibodies are shown. (B) Yeast two hybrid assays of yeast co-transformed with either pGAD vector (V) or pGAD-PAR-5 and pGBD containing the various LET-99 constructs shown to the right. Red lines indicate the positions of predicted 14-3-3 binding domains at amino acids 121-126, 245-250,269-274, 317-323 and 515-520. Equal amounts of cultures grown to an OD of 0.5 were spotted on plates without histidine for vector and PAR-co-transformants, along with two dilutions of PAR-5 co-transformants (see Methods). Growth was scored as (+++) if all dilutions grew robustly, and (-) if growth was similar to controls; the score shown is an average of two replicates.

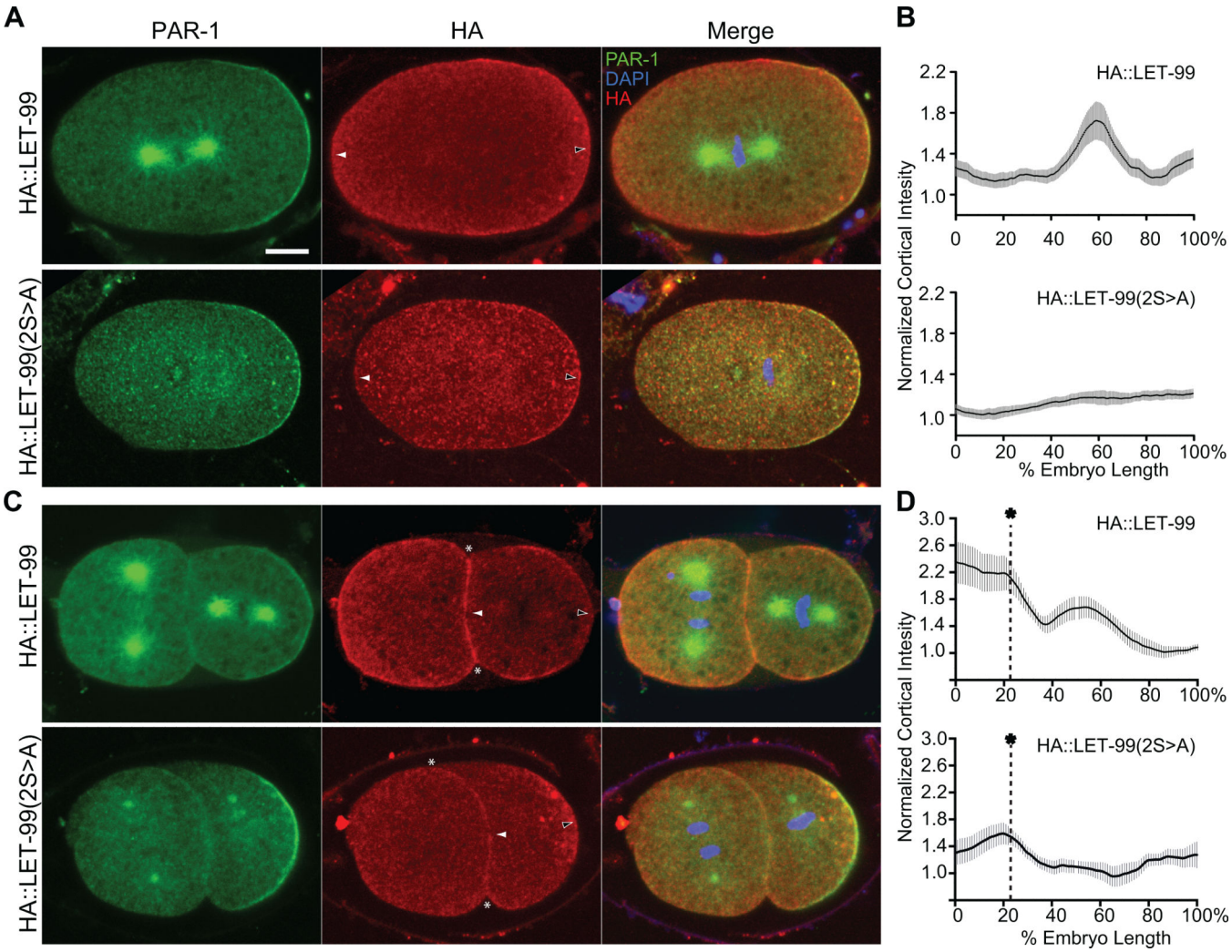

Fig. 3.

PAR-5 binding sites are required for LET-99 localization. (A) Confocal images of PAR-1 and HA localization in one-cell embryos expressing HA::LET-99 and HA::LET-99 (2S>A). Merged images to right are combined with DAPI to mark the chromosomes. Arrowheads mark the beginning (0%EL, white,) and ending (100%EL, open white) positions of the cortical trace. (B) Plots showing the average cortical intensities of HA localization in one-cell embryos with detectable cortical signal. For RL269 HA::LET-99, n=10 and, for RL193 HA::LET-99(2S>A), n=13. Error bars are standard error of the mean. (C) Confocal images of PAR-1 and HA localization in two-cell embryos. Arrowheads mark the beginning (0%EL, white,) and ending (100%EL, open white) positions of the cortical trace; astericks mark the end of the cell contact. (D) Plots showing the average cortical intensities of HA localization in P1 of two-cell embryos; n=5 each for RL269 HA::LET-99 and RL193 HA::LET-99(2S>A). Dashed lines corresponds to position of astericks in images. Error bars are standard error of the mean. Scale bar: 10 μm.

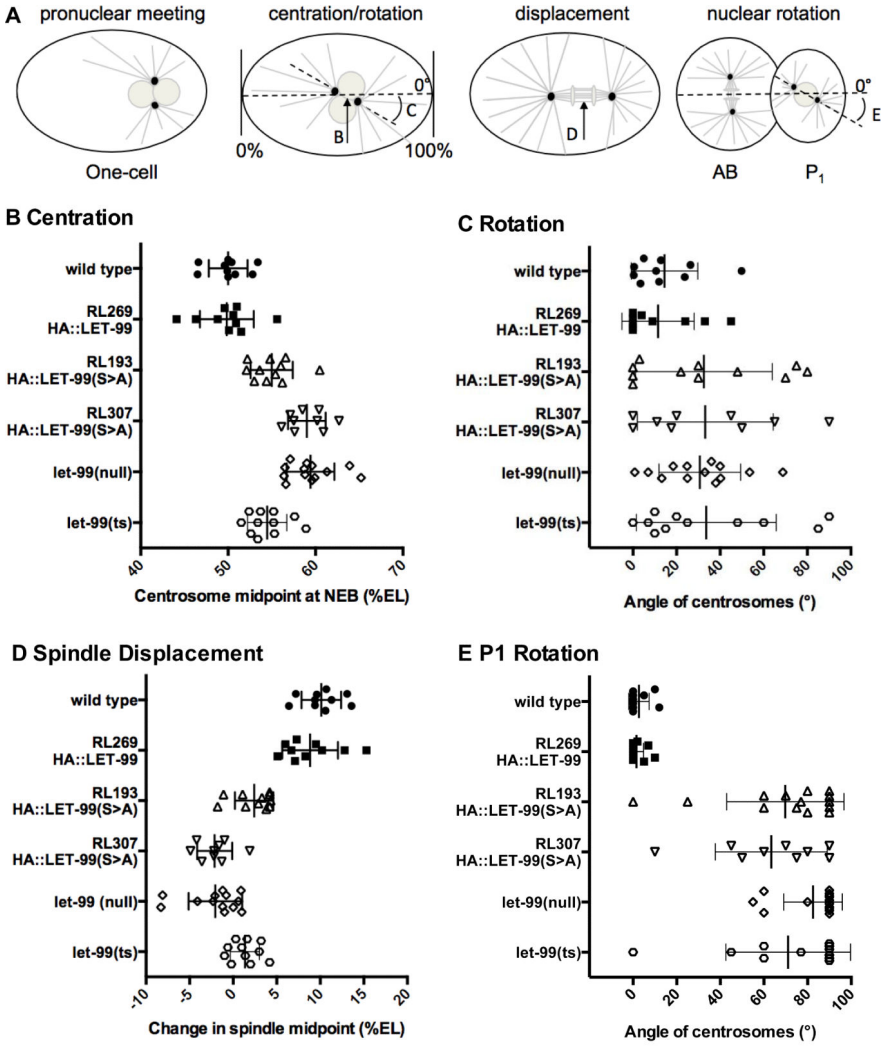

F

Genotype	N	Centration (%EL)	One-cell rotation angle (°)	Spindle Displacement (%EL)	Two-cell P1 rotation angle (°)
wild type	10	50.0 ± 0.7	14.5 ± 4.8	10.1 ± 0.7	2.7 ± 1.5
RL269, HA::LET-99	10	49.9 ± 1.0	11.5 ± 5.2	8.8 ± 1.0	1.6 ± 0.8
RL193, HA::LET-99(S>A)	11	55.0 ± 0.7 [a,b]	32.6 ± 9.5	2.4 ± 0.7 [a,b]	69.8 ± 7.1 [a,b]
RL307, HA::LET-99(S>A)	9	59.0 ± 0.7 [a,b,c]	29.2 ± 10.9	-2.1 ± 0.7 [a,b,c]	63.3 ± 8.5 [a,b]
let-99(null)	13	59.4 ± 0.8 [a,b,c]	30.7 ± 5.2 [a,b]	-2.0 ± 0.9 [a,b,c]	82.5 ± 3.6 [a,b]
let-99(ts)	11	54.5 ± 0.7 [a,b]	35.5 ± 10.5	1.4 ± 0.5 [a,b]	71.1 ± 8.6 [a,b]

Fig. 4.

Quantification of nuclear and spindle movements in early embryos. (A) Schematic diagram of nuclear and spindle movements during the one and two-cell stages; anterior is to the left and posterior to the right in all diagrams. The letters correspond to the measurements shown in each of the scatter plots (B-E). In each plot, means are indicated by thick vertical lines and standard deviations with thin vertical lines. (B) Midpoint of the nuclear-centrosome complex at NEB, expressed as percent embryo length (%EL) (C) Rotation angle of nuclear-centrosome complex at NEB, where the AP axis = 0°. (D) Displacement of the spindle,

measured as the change in midpoint between the two centrosomes from NEB to the onset of cytokinesis. (E) Rotation angle of P1 nuclear-centrosome complex at NEB, AP axis = 0°. (F) Means +/− standard deviation for each genotype and measurement shown. The number of embryos (N) refers to the one-cell stage; more were analyzed for P1 rotation. Statistically different values are indicated: [a] statistically different from wild-type, $p<0.05$; [b] statistically different from RL269, $p<0.05$; [c] statistically different from RL193, $p<0.05$. Not shown for simplicity: *let-99(ts)* was also statistically different from RL307 and *let-99(null)* for centration and displacement; *let-99(null)* was only different from RL307 for P1 rotation.